Journal of Power Sources 196 (2011) 1048–1054

Contents lists available at ScienceDirect

Journal of Power Sources

journal homepage: www.elsevier.com/locate/jpowsour

Fast proton-conducting glass membrane based on porous phosphosilicate and perfluorosulfonic acid polymer

Fengjing Jiang, Zhigang Di, Haibin Li*, Hengyong Tu, Qingchun Yu

Institute of Fuel Cell, School of Mechanical Engineering, Shanghai Jiao Tong University, 800 Dongchuan Road, Shanghai 200240, China

ARTICLE INFO

Article history:
Received 13 June 2010
Received in revised form 5 August 2010
Accepted 9 August 2010
Available online 17 August 2010

Keywords:
Proton-conducting glass
Hybrid membrane
Phosphosilicate
Fuel cell

ABSTRACT

A proton-conducting glass membrane based on porous phosphosilicate and perfluorosulfonic acid polymer was prepared via a modified sol–gel approach. The morphology, pore structure, water uptake property, proton conductivity and fuel cell performance of the membrane were investigated in this work. The hybrid glass membrane showed extremely high proton conductivity of 0.1 S cm^{-1} in humid atmosphere. In the H_2/O_2 fuel cell measurement, an open circuit potential (OCV) of 0.94 V and a maximum output power density of 42.6 mW cm^{-2} was obtained at 25 °C.

1. Introduction

Proton exchange membranes (PEMs) for fuel cells have undergone significant developments during the past decades [1–12]. The current state-of-the-art proton electrolyte membranes for polymer electrolyte membrane fuel cell (PEMFC) with the operating temperature below 100 °C are perfluorinated sulfonic acid ionomers such as Nafion® [13,14]. Nafion® has received a considerable amount of attention as a proton conductor because of its high proton conductivity, excellent thermal and mechanical stability. Nevertheless, Nafion® has certain limitations. It is a water based proton conductor which falls dry quickly at temperatures above 80 °C due to evaporation of water from the polymer matrix. Nafion® membrane in a fuel cell suffers from the stress which caused by the swelling and deswelling of the membrane in humid atmosphere and therefore, may bring damages to the membrane. Moreover, the methanol permeability of Nafion® membrane is too high to be used in direct methanol fuel cells (DMFC).

Nogami et al. have proposed the sol–gel preparation of inorganic glass membranes with a promising proton conductivity of 10 mS cm^{-1} at room temperature [15,16]. Various of inorganic proton conductive glasses including acid/glass hybrids have been prepared and investigated [17–19]. However, most of the acids are both water and alcohol soluble, as a result, their applications are limited. Inorganic glass membrane exhibits excellent thermal stability at the temperatures above 400 °C and no decrease of conductivity is observed up to 120 °C [20]. The advantages of high proton conductivity, excellent thermal stability and low cost make the inorganic glasses very promising to substitute polymer electrolytes for the practical application in fuel cells. However, most of the inorganic glasses, such as P_2O_5–SiO_2 glasses, show deficient flexibility for the membrane electrode assembling as well as the fuel cell assembling. Thus, the feasibility of the application of inorganic glass in fuel cells is challenged because of its brittleness. The idea of combining inorganic glass and perfluorosulfonic acid polymer was promoted by Nogami et al. with the purpose of improving the flexibility of the glass [21].

Recently, we proposed a novel approach (hydrothermal treatment) to anneal the phosphosilicate gel at a much lower temperature (below 150 °C) than the conventional method (above 400 °C). As a result, the hydrothermal-treated phosphosilicate glass membrane showed a surprisingly high proton conductivity of 0.211 S cm^{-1} at 90 °C (70% relative humidity). The hydrothermal treatment process makes possible to prepare polymer/glass hybrids via a sol–gel method avoiding thermal degradation of the organic component which happens at high temperatures.

To the best of our knowledge, most of the proton conductive inorganic glasses have a porous structure with the pore size ranging from several to decades of nanometers which is essential for proton transfer within the glass. However, the porous structure may cause an inevitable problem of fuel leaking through the membrane which has been observed in our previous study.

In our search for solving the problem of fuel leaking, we found that the combination of proton conductive polyelectrolyte and inorganic glass with an appropriate ratio could be an effective approach. The polyelectrolyte could play a role of pore filler to

* Corresponding author. Tel.: +86 21 34206249, fax: +86 21 34206249.
E-mail address: haibinli@sjtu.edu.cn (H. Li).

0378-7753/$ – see front matter © 2010 Elsevier B.V. All rights reserved.
doi:10.1016/j.jpowsour.2010.08.030

Table 1
Sample names and the corresponding component.

File name of the sample	Si:P in glass (molar ratio)	Feed ratio of TEOS:Nafion® (weight ratio)
NPSi-1	9:1	9:1
NPSi-2	8:2	9:1
NPSi-3	7:3	9:1
NPSi-4	9:1	8:2
NPSi-5	8:2	8:2
NPSi-6	9:1	7:3
NPSi-7	8:2	7:3

reduce the fuel permeation. Moreover, the polymer should be highly proton conductive in order to avoid notable interruption of proton diffusion. Following the seminal work of Nogami et al. [21], we have prepared the composite of phosphosilicate glass and perfluorosulfonic acid polymer using a modified sol–gel process. The morphology, pore structure, water uptake property, proton conductivity and fuel cell performance of the membrane will be discussed.

2. Experimental

2.1. Material

$Si(OC_2H_5)_4$ (TEOS, Sinopharm, Analytical reagent), H_3PO_4 (85% aqueous solution, Sinopharm) and Nafion® perfluorinated ion-exchange resin (Aldrich, 5 wt.% solution in a mixture of lower aliphatic alcohols and water) were used without further purification.

2.2. Preparation of polyelectrolyte/phosphosilicate glass membrane

The glass membranes were prepared via a optimized sol–gel method. The sample names of the obtained Nafion®/phosphosilicate glasses and their components were listed in Table 1. The details of the preparation was described as following.

A mixture of TEOS, deionized water and hydrochloric acid in the molar ratio of $1{:}4{:}4 \times 10^{-3}$ ($TEOS{:}H_2O{:}HCl$) was firstly prepared and stirred for 30 min at room temperature. Then, certain amount of Nafion® and phosphoric acid solution was slowly added to the mixture above with a further stirring of 20 min. The obtained transparent was then transferred into a Teflon vessel and aged at room temperature until gelation happens. Hydrothermal treatment of the Nafion®/phosphosilicate gels was taken place by annealing them at 150 °C for 24 h under saturated water vapor.

2.3. Characterization of the Nafion®/phosphosilicate glasses

Images of samples were captured by using a digital camera (DSC-W50, Sony). The porous structure of the glass membranes was analyzed by nitrogen adsorption–desorption apparatus (ASAP 2010 M+C, Micromeritics Inc.) after degassing at 150 °C.

The proton conductivity was measured by dielectric spectroscopy in a two-electrode geometry using an SI 1260 impedance/gain-phase analyzer in the frequency range of 10^{-1} to 10^6 Hz (SI-1260, Solartron). The samples used for proton conduction test were membranes with the thickness of 0.2–0.5 mm thick. Parallel gold electrodes were sputtered on the glass membranes through a shadow mask. Electrical contacts to both electrodes were made with soldered Au wires. Proton conductivities were evaluated from Cole–Cole plots [22].

Conductivities of the samples are calculated from the following formula:

$$\sigma = \frac{L}{AR} \quad (1)$$

where R is determined from the semi-circle response on the real axis of the complex impedance plot, L represents the thickness of the sample film, and A is the area of top Au electrode.

The temperature and humidity of air during data acquisition was set by a constant temperature and humidity chamber (LHS-100CL, BLUE PARD). In order to determine the amount of water sorption, the samples were stored under an atmosphere of fixed relative humidity at 50 °C for 2 days. The uptake of water was measured on a micro-balance until constant weight W was obtained; the water sorption was calculated from Eq. (2).

$$\text{water uptake } (\%) = \frac{W_{\text{wet}} - W_{\text{dry}}}{W_{\text{dry}}} \times 100 \quad (2)$$

Thermal gravimetric analysis (TGA) was obtained using the TGA-2050 instruments under a N_2 flow of 60 ml min^{-1} with a heating rate of 10 K min^{-1}.

Scanning electron microscopy (SEM) images were obtained on field emission SEM (JSM-7600F, JEOL) which allows obtaining images with high magnification at low operating voltages.

2.4. Membrane electrode assembly (MEA) and H_2/air fuel cell test

The catalyst ink was prepared by the mixing of a Nafion® solution (Aldrich, 5 wt% solution in a mixture of lower aliphatic alcohols and water), Pt/C (60%Pt/C, Johnson Matthey), polytetraflouroethylene (PTFE) and glycol with a weight ratio of 0.5:1:0.2:6 (Nafion®:Pt/C:PTFE:glycol). The mixture was stirred under magnetic stirring for 30 min and then ultrasonic dispersed for 5 min. The electrodes were then prepared by spraying the catalyst ink onto the wet-proofed carbon paper (2050-A, Ballard, with gas diffusion layer) and dried at 120 °C under reduced pressure for 24 h to completely remove the solvents. The Pt loading used for the electrodes was 1.46 mg cm^{-2}. After that, the MEA was made by attaching the electrodes onto the glass membrane using dilute Nafion® solution (10 wt% solution in a mixture of lower aliphatic alcohols and water) as an adhesive. The active surface area of the MEA used for the fuel cell test was 0.5 cm^2.

The H_2/air fuel cell was fuelled with pure hydrogen supplied onto the anode and air onto the cathode at 1 atm. The gas flow and humidification were controlled by a fuel cell testing system (CHINO, Japan). The polarization curves and impedance data were collected using a Solartron-1287 electrochemical interface and a Solartron-1260 impedance analyzer in the frequency range of 10^{-1} to 10^6 Hz.

3. Results and discussion

3.1. Morphology and structure of Nafion®/phosphosilicate glasses

With the modified sol–gel approach, homogenous and crack-free Nafion®/phosphosilicate hybrid glass membranes were obtained (see Fig. 1). The shape and size of the membrane can be controlled by changing the shape of the vessel in which the membrane is made. The thickness of the membrane can be as thin as 200 μm. The hybrid membrane treated via the conventional method (annealing at high temperatures above 300 °C) was easily getting cracked and the color of the membrane turned to be dark brown or black due to the degradation of the polymer. According to the TGA analysis in Fig. 2, the membranes are thermally unstable above 270 °C. The TGA curves shown in Fig. 2 are typical TGA curves of Nafion according to a thermal degradation study of Nafion [23].

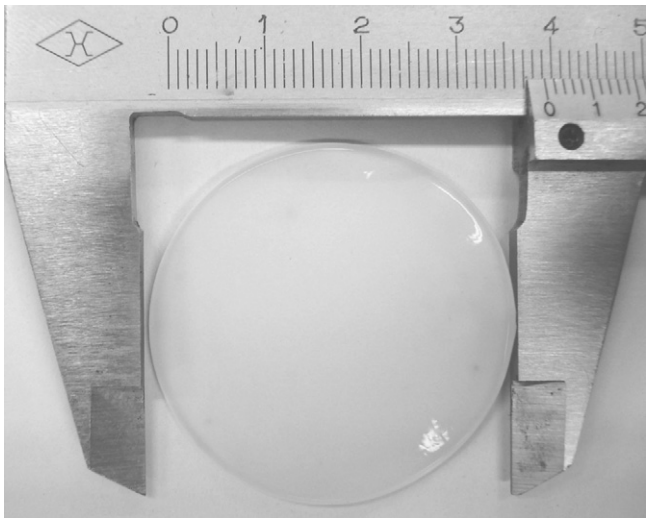

Fig. 1. Digital photo of Nafion®/phosphosilicate hybrid glass membrane.

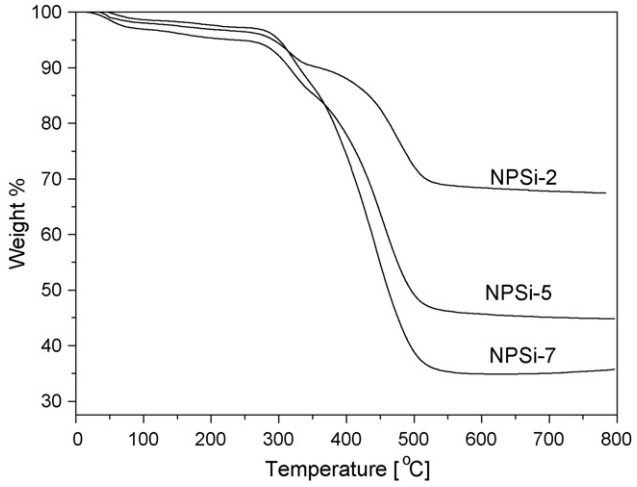

Fig. 2. TGA curves of the hybrid glass membranes.

The morphology of the Nafion®/phosphosilicate glass membranes was observed by field emission SEM. Fig. 3 shows the SEM images of NPSi-1 (a), NPSi-2 (b), NPSi-3 (c) and NPSi-6 (d), respectively. It is apparent that the hybrid membrane consists of nanoparticles (a few nanometers in diameter) with porous structure. The SEM images indicate the homogeneous structure of the membrane and no aggregations of polymer can be observed. The polyelectrolyte is entrapped within and highly dispersed throughout the SiO_2 network. The homogeneous structure of the SiO_2 framework and the highly dispersed polymer filler also give the hybrid glass membrane an enhanced mechanical property which is important for the membrane electrode assembly.

The surface of all the Nafion®/phosphosilicate glass membranes has the pore size ranging from several to decades of nanometers. The pore size increases notably as the H_3PO_4 content increases (compare Fig. 3a–c). Fig. 3d shows the morphology of NPSi-6 which has the same molar ratio of H_3PO_4 to TEOS as NPSi-1. Compared with Fig. 3a, NPSi-6 membrane seems less porous than NPSi-1 because NPSi-6 contains more Nafion® than NPSi-1 (see Table 1) where the polymer plays a role of pore-filler in the hybrids.

3.2. Pore structure of the hybrid glass membranes

The porous structure of the hybrid glass membranes were evaluated by N_2 adsorption–desorption isotherms and BJH pore size distribution plot. Fig. 4 shows the pore-size distribution curves determined by BJH equation using the desorption branch of the N_2 gas adsorption–desorption isotherms. In Fig. 4(a), NPSi-1, NPSi-2 and NPSi-3 have the average diameter of 13.2, 15.4 and 17.5 nm, respectively. Along with the increase of H_3PO_4 content, the average pore diameter of the membrane increases. This result was in accordance with the SEM analysis which further proved that H_3PO_4 concentration has influence on the pore distribution of the glass membranes. The average pore size of the membrane increases with H_3PO_4 concentration. In Fig. 4(b), the average diameter of NPSi-1,

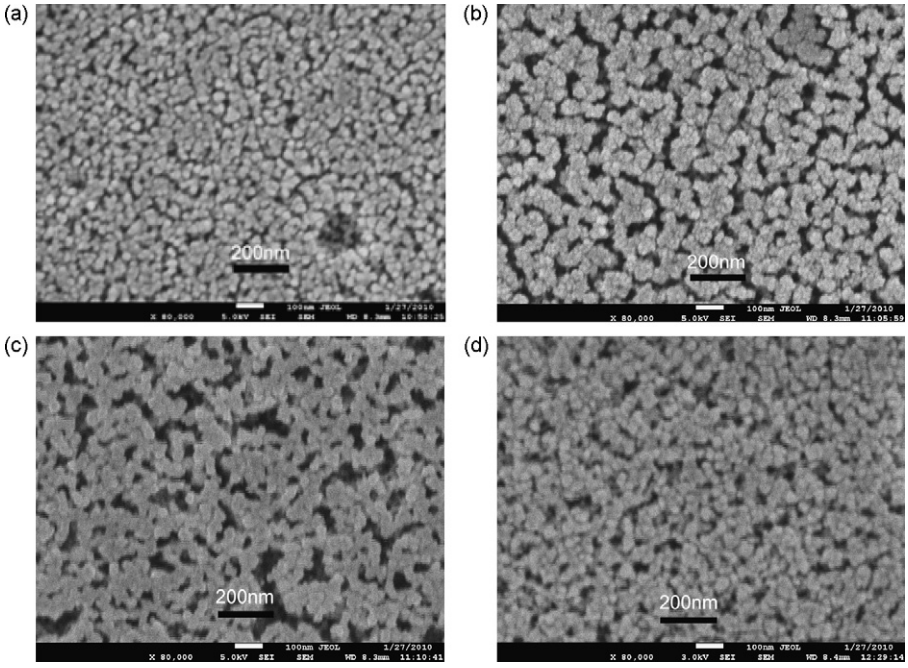

Fig. 3. SEM images of NPSi-1 (a), NPSi-2 (b), NPSi-3 (c) and NPSi-6 (d), respectively.

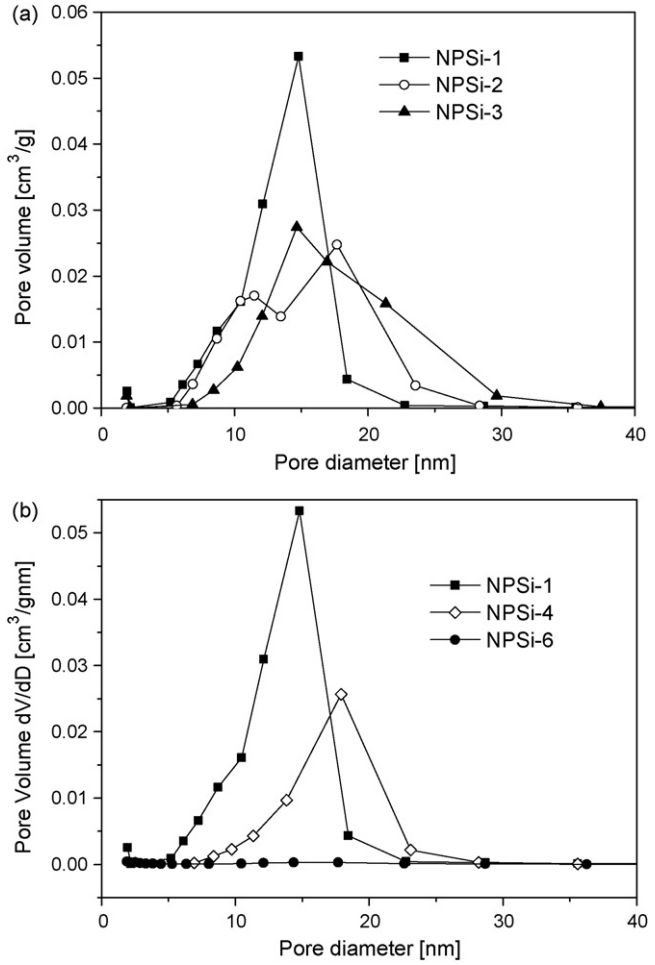

Fig. 4. The pore-size distribution curves determined by BJH equation using the desorption branch of the N_2 gas adsorption–desorption isotherms.

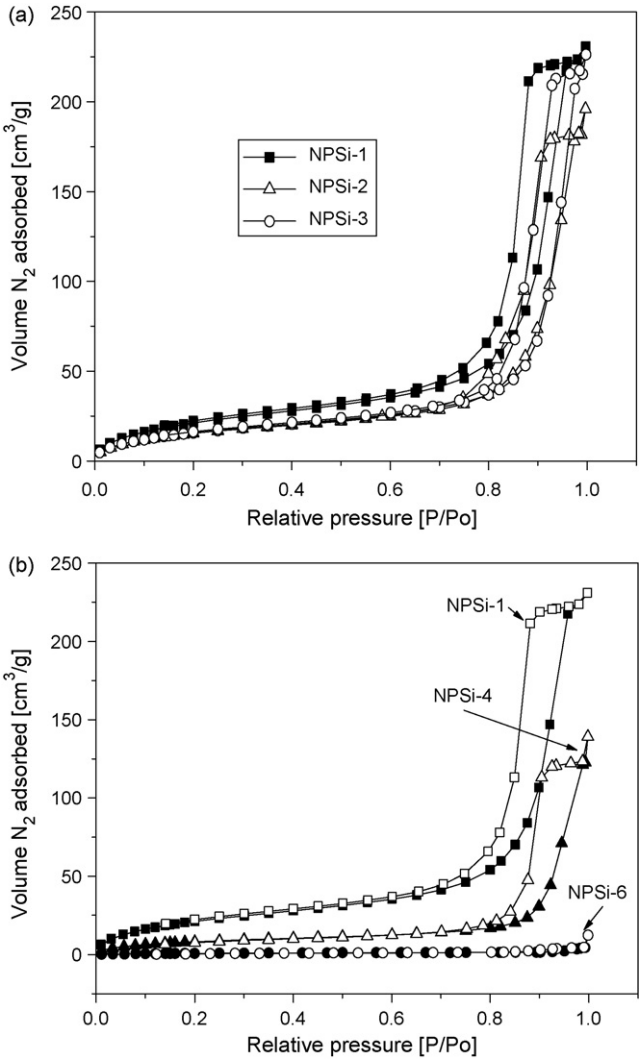

Fig. 5. N_2 adsorption–desorption isotherms. Solid and hollow marks indicate the adsorption and desorption branches, respectively.

NPSi-4 and NPSi-6 are 13.2, 18.6 and 31.6 nm, respectively. Along with the increase of Nafion® content, the average pore diameter of the membrane increases. The reason is not clear yet. A possible explanation would be that most of the small pores are filled with Nafion and the large pores remain which leads to an increase in average pore diameter. The total pore volume (0.36, 0.22 and 0.02 $cm^3\ g^{-1}$ for NPSi-1, NPSi-4 and NPSi-6, respectively) decreases dramatically with increasing Nafion® content because Nafion® acts as pore filler in the porous glass matrix as is expected. The optimized structure of the hybrid membrane which can be controlled by changing the amount of H_3PO_4 and Nafion® is crucial for the high performance hybrid membrane.

In N_2 adsorption–desorption isotherms, the width of the hysteresis indicates the accessibility of the pores. Normally, the wider is the hysteresis, the more interconnected are the pores [24]. In bare phosphosilicate glass membrane, the interconnection between pores is indispensable for achieving high proton conductivity. However, the interconnected pore may leads to severe fuel leakage. In the Nafion®/phosphosilicate hybrid membrane, Nafion® was introduced to reduce the pore volume without notable sacrifice in proton conductivity. In Fig. 5(a), NPSi-1, NPSi-2 and NPSi-3 shows similar hysteresis which indicate that H_3PO_4 has inconspicuous effect on pore connectedness. In Fig. 5(b), the pore interconnection of NPSi-4 is similar with that of NPSi-1 which demonstrates that the Nafion® content in NPSi-4 is not sufficient to block the interconnection of the pores. In NPSi-6, most of the pores are filled up with Nafion®, and therefore, no pore interconnection can be observed.

3.3. Water uptake property of the hybrid glass membrane

Water uptake property of the hybrid glass membranes was compared in Figs. 6 and 7. The samples for both water uptake and conductivity measurements were placed simultaneously in the constant temperature and humidity chamber. Fig. 6 shows the water uptake property of NPSi-1, NPSi-2 and NPSi-3 under various relative humidity measured at 50 °C. We can see that, the membrane with more H_3PO_4 content is more hygroscopic. The discrepancy is notable at high relative humidity. In Fig. 7, the water uptake property of the glass membranes with different Nafion® content was compared. We can see that the water uptake of the membranes decreases with increasing Nafion® content. This is because the pore volume of the hybrid membrane decreases with increasing Nafion content and the amount of water that can be adsorbed by the membrane is heavily depended on the pore volume of the membrane.

3.4. Proton conductivity of the hybrid glass membrane

Fig. 8 shows the proton conductivities of the hybrid glass membranes against relative humidity at 50 °C. We can see that the increasing water content (see the water uptake data displayed in Fig. 6) leads to rapidly increase in conductivity. NPSi-3 shows the

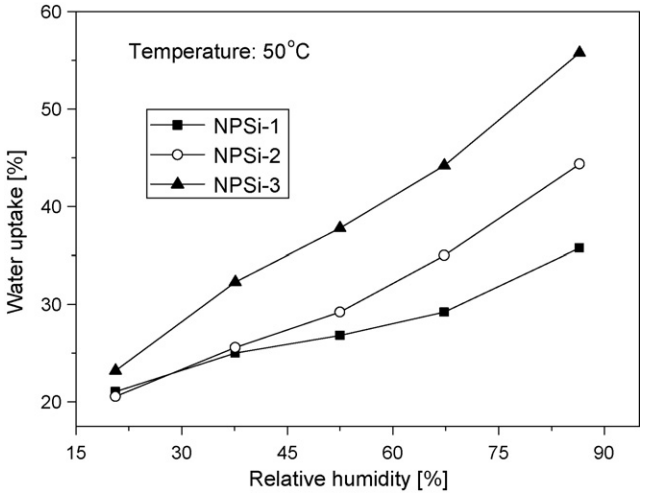

Fig. 6. Water uptake of NPSi-1, NPSi-2 and NPSi-3 under various relative humidity.

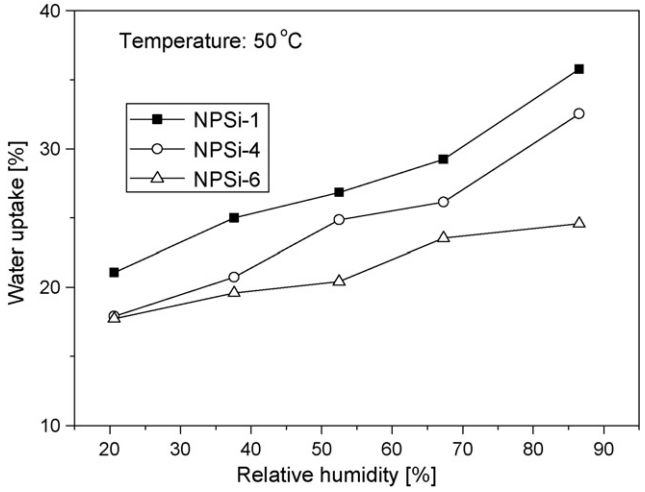

Fig. 7. Water uptake of NPSi-1, NPSi-4, NPSi-6 under various relative humidity.

highest proton conductivity which can reach 0.1 S cm^{-1} with 85% relative humidity, at 50 °C. The membranes show high proton conductivity even at 20% relative humidity (>10^{-3} S cm^{-1}). From 20 to 85% relative humidity, the conductivity of NPSi-3 increases from

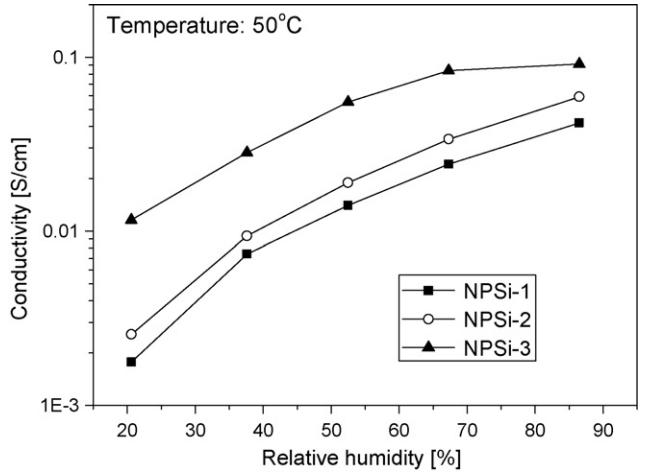

Fig. 8. Proton conductivities of NPSi-1, NPSi-2 and NPSi-3 against relative humidity at 50 °C.

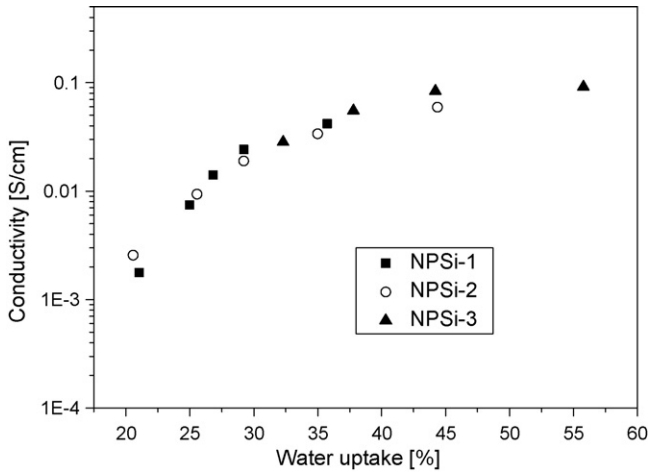

Fig. 9. Plot of conductivity versus water content in the hybrid glass membranes (at 50 °C).

0.01 to 0.1 S cm^{-1}. Conductivities of the three membranes increase rapidly with relative humidity which indicates that water is significantly important for proton transport in these membranes. Fig. 8 shows the apparent effect of H_3PO_4 content on proton conductivity when plotted against relative humidity. However, the fact how H_3PO_4 content influences the proton conductivity of the membrane cannot be read from the data in Fig. 8. In Fig. 9, we plotted the conductivity versus water content (water uptake) in the glass membrane based on the data in Figs. 6 and 8. Interestingly, a "master curve" of the relation between proton conductivity and water content can be obtained for the membranes with the same Nafion® content. It is demonstrated that, with the water uptake higher than 20%, proton conduction is a water-governed process which happens in the water salvation. Proton conductivity is exclusively determined by water content in the membranes, where the direct effect of underlying structure and composition of the membrane on proton conduction can be neglected. This phenomenon was also observed in previous reported work [6].

Proton conductivities of NPSi-1, NPSi-4 and NPSi-6 under various relative humidity were measured at 50 °C. The result was shown in Fig. 10. We can see that NPSi-4 shows higher proton conductivity than NPSi-1, though NPSi-4 is less hygroscopic. As discussed above, water plays an important role on proton conduction in the membrane. Therefore, a lower proton conductivity of NPSi-

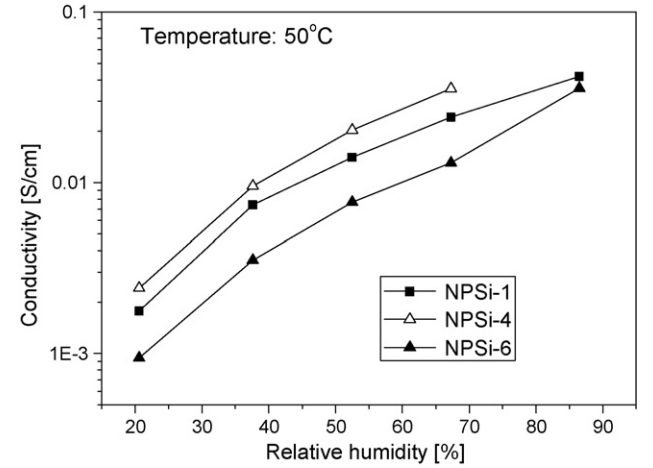

Fig. 10. Proton conductivities of NPSi-1, NPSi-4 and NPSi-6 against relative humidity at 50 °C.

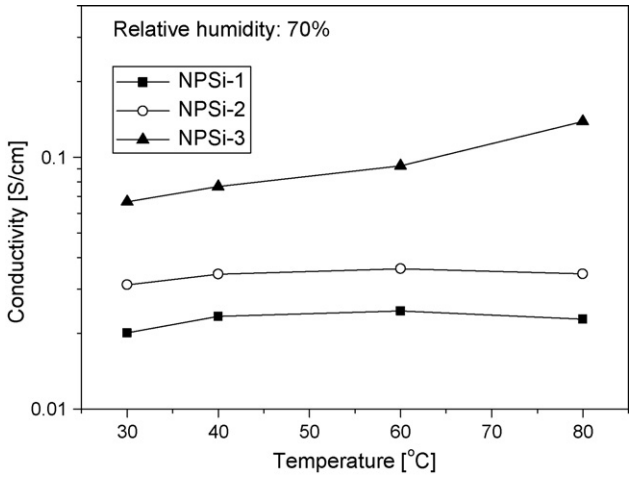

Fig. 11. Temperature dependence of proton conductivities of NPSi-1, NPSi-2 and NPSi-3 measured with 70% relative humidity.

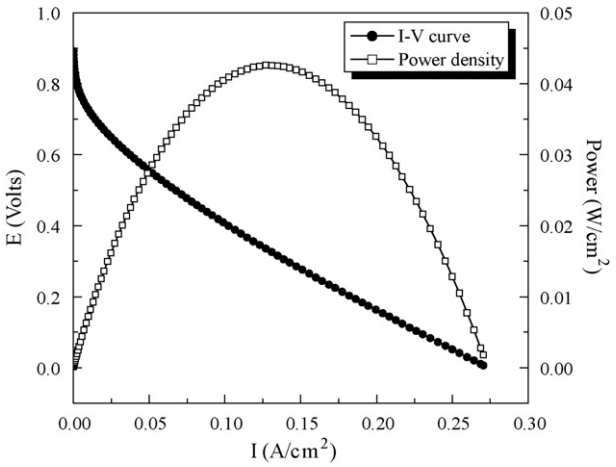

Fig. 12. Power density derived from *I–V* curve for NPSi-3 based fuel cell at room temp.

4 than NPSi-1 should be expected according to the water uptake property shown in Fig. 7. However, Nafion® itself is a fast proton conductor and could promote proton conduction of the hybrid membranes. The overall effect of Nafion® on proton conductivity depends on its content in the hybrid membranes. For example, in NPSi-4 where the feed ratio of Nafion® to TEOS is 1:4, Nafion® shows positive effect on proton conductivity as compared with NPSi-1. However, in NPSi-6, the water uptake of the membrane is significantly lowed by increasing the Nafion® content in the hybrid membrane, and this became the dominant effect on proton conductivity, therefore, NPSi-6 shows the lowest proton conductivity among the three membranes.

Fig. 11 demonstrates the temperature dependence of proton conductivities of NPSi-1, NPSi-2 and NPSi-3 measured with 70% relative humidity. All the membranes possess promising proton conductivity (above 0.01 S cm^{-1}) during the measuring temperature range. Notably, NPSi-3 shows extremely high proton conductivity of about 0.07 S cm^{-1} at 30 °C, 70% relative humidity and exceeds 0.1 S cm^{-1} at 80 °C, 70% relative humidity.

3.5. H_2/air fuel cell testing

The H_2/air fuel cell test was carried out with humidified H_2 and air fed into anode and cathode respectively at room temperature. The gas flow rates of H_2 and air were 20 and 100 sccm, respectively. Based on the consideration of conductivity and fuel permeation, the sample of NPSi-3 was selected for fuel cell testing.

The open circuit voltage of the fuel cell was maintained at 0.94 V after a period of constant fuel supplement and cyclic activation. Polarization curve was then recorded to show the overall performance of the fuel cell, as shown in Fig. 12. Power density was simultaneously derived from the *I–V* curve. A drop of the cell voltage even under a initial small load current shows a great activation potential loss which can be frequently observed at low operating temperatures. The obtained power density was 42.6 mW cm^{-2}.

An impedance analysis of the MEA was carried out with a voltage load of 0.4 V and the impedance spectra is shown in Fig. 13. The ohmic resistance (R_Ω) of the fuel cell shown in Fig. 13 was 1.27 Ωcm^2 which consists the electronic resistance and the membrane resistance. An estimation of the proton conductivity of the membrane can be made using the following equation:

$$\sigma = \frac{L}{\mathrm{ASR}} \tag{3}$$

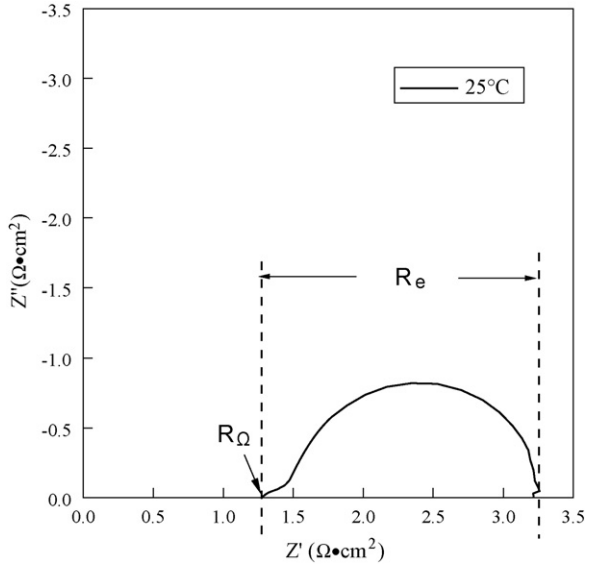

Fig. 13. Impedance spectra of NPSi-3 based fuel cell at 0.4 V.

where σ is the proton conductivity of the membrane, L and ASR are the thickness and area specific resistance of the membrane, respectively. The thickness of the used membrane was around 0.5 mm. Suppose ASR of the membrane is 1.27 Ωcm^2 (ignoring the electronic resistance), the calculated conductivity was around 0.04 S cm^{-1} which is in accordance with that discussed in Section 3.4.

The indicated total electrode resistantce (R_e) of both the cathode and the anode is about 2 Ωcm^2 which is rather high as compared with that of Nafion® based MEA. The electrode resistance can be effectively reduced by optimizing the structure and component of the elctrode. This work is still undergoing and will be reported later.

Based on the promising proton conductivity, this membrane could be possibly used as novel proton exchange membranes in fuel cells. Another possible application for this kind membrane is to be used in humidity sensors.

4. Conclusion

Fast proton-conducting glass membranes based on phosphosilicate glass and Nafion® were prepared using a modified sol–gel approach. The hybrid membranes show very promising proton con-

ductivity which can exceed 0.1 S cm^{-1}. With fixed Nafion® content, proton conductivity of the hybrid membrane is exclusively determined by water content in the membrane. Nafion® can reduce the pore volume notably while enlarging the pore size of the glass membrane. The glass membrane is also found to be strong mechanically and thermally stable through the structural and thermal studies. The single H_2/air fuel cell equipped with the prepared hybrid glass membrane shows a stable open cell voltage of 0.94 V and a power density of 42.6 mW cm^{-2} can be obtained.

Acknowledgements

This work was supported by Shanghai Pujiang Program (Grant No. 08PJ1406500), the International Science & Technology Cooperation Program (Grant No. 2008DFA51200), the National High-Tech R&D Program (863 Program) (Grant No. 2009AA05Z113), and the National Natural Science Foundation of China (Grant No. 50672058).

References

[1] F. Jiang, H. Pu, W.H. Meyer, Y. Guan, D. Wan, Electrochim. Acta 53 (2008) 4495–4499.
[2] S. Bhadra, N.H. Kim, J.H. Lee, J. Membr. Sci. 349 (2010) 304–311.
[3] M.D. Robert, H.L. Morgan, M.I. Richard, J. Power Sources 195 (2010) 6405–6410.
[4] H. Li, G. Zhang, J. Wu, C. Zhao, Y. Zhang, K. Shao, M. Han, H. Lin, J. Zhu, H. Na, J. Power Sources 195 (2010) 6443–6449.
[5] M.A. Abdelkareem, T. Tsujiguchi, N. Nakagawa, J. Power Sources 195 (2010) 6287–6293.
[6] F. Jiang, A. Kaltbeitzel, B. Fassbender, G. Brunklaus, W.H. Meyer, H.W. Spiess, G. Wegner, Macromol. Chem. Phys. 209 (2008) 2494–2503.
[7] A.C. Fernandes, E.A. Ticianelli, J. Power Sources 193 (2009) 547–554.
[8] D. Zhao, B. Yi, H. Zhang, H. Yu, J. Power Sources 195 (2010) 4606–4612.
[9] F. Jiang, H. Zhu, R. Graf, W.H. Meyer, H.W. Spiess, G. Wegner, Phase Behavior, Macromolecules 43 (2010) 3876–3881.
[10] M. Schuster, W.H. Meyer, G. Wegner, H.G. Herz, M. Ise, K.D. Kreuer, J. Maier, Solid State Ionics 145 (2001) 85–92.
[11] F. Jiang, A. Kaltbeitzel, W.H. Meyer, G. Wegner, Macromolecules 41 (2008) 3081–3085.
[12] H. Kim, S. Prakash, W.E. Mustain, P.A. Kohl, J. Power Sources 193 (2009) 562–569.
[13] M.K. Verbrugge, R.F. Hill, J. Electrochem. Soc. 137 (1990) 3770–3777.
[14] K.D. Kreuer, Solid State Ionics 97 (1997) 1–15.
[15] M. Nogami, H. Matsushita, Y. Goto, T. Kasuga, Adv. Mater. 12 (2000) 1370–1372.
[16] M. Nogami, R. Nagao, C. Wong, T. Kasuga, T. Hayakawa, J. Phys. Chem. B 103 (1999) 9468–9472.
[17] T. Uma, M. Nogami, ChemPhysChem 8 (2007) 2227–2234.
[18] T. Kasuga, M. Nakano, M. Nogami, Adv. Mater. 14 (2002) 1490–1492.
[19] H. Li, M. Nogami, Adv. Mater. 14 (2002) 912–914.
[20] K. Daiko, T. Kasuga, M. Nogami, J. Ceram. Soc. Jpn. 109 (2001) 815–817.
[21] M. Nogami, Y. Usui, T. Kasuga, Fuel cells 1 (2002) 181–185.
[22] J.G. Powles, Proc. Phys. Soc. B 64 (1951) 81–82.
[23] Q. Deng, C.A. Wilkie, R.B. Moore, K.A. Mauritz, Polymer 39 (1998) 5961–5972.
[24] M.T.N. Colomer, Adv. Mater. 18 (2006) 371–374.